Title: Design of a Minimal di-Nickel Hydrogenase Peptide

Authors: Joshua A. Mancini[1,2†], Douglas H. Pike[2†], Saroj Poudel[1,2†], Jennifer Timm[1,2†], Alexei M. Tyryshkin[1,2†], Jan Siess[2], Paul Molinaro[3], James J. McCann[3], Kate M. Waldie[4], Ronald L. Koder[3], Paul G. Falkowski[1*], and Vikas Nanda[2*]

Affiliations:

[1]Environmental Biophysics and Molecular Ecology Program, Department of Marine and Coastal Sciences and the Department of Earth and Planetary Sciences, Rutgers University, New Brunswick, NJ 08901, US.

[2]Center for Advanced Biotechnology and Medicine and the Department of Biochemistry and Molecular Biology, Robert Wood Johnson Medical School, Rutgers University, Piscataway, NJ 08854, US.

[3]Department of Physics, The City College of New York, New York, NY 10016, US.

[4]Department of Chemistry and Chemical Biology, Rutgers University, Piscataway, NJ 08854, US.

[†]contributed equally

[*]correspondence: falko@marine.rutgers.edu, vik.nanda@rutgers.edu

Abstract:

The most ancient processes for energy production in the evolution of life involve the reversible oxidation of molecular hydrogen by hydrogenase. Extant hydrogenase enzymes are complex, comprising hundreds of amino acids and multiple cofactors. We designed a 13 amino acid nickel-binding peptide capable of robustly producing molecular hydrogen from protons under a wide variety of conditions. The peptide forms a di-nickel cluster structurally analogous to a Ni-Fe cluster in [NiFe]-hydrogenase and the Ni-Ni cluster in acetyl-CoA synthase (ACS), two ancient, extant proteins central to metabolism. These experimental results clearly demonstrate that modern enzymes, despite their enormous complexity, likely evolved from simple peptide precursors on early Earth.

One Sentence Summary: Small metal-binding peptides were the likely precursors of modern enzymes.

Main Text:

In the contemporary world, molecular hydrogen (H_2) is only used as a source of energy by specialized microorganisms in anaerobic environments, but early in Earth's history, the first microbial metabolisms were almost certainly dependent on H_2 (*1, 2*). Reversible biological oxidation of H_2 is catalyzed by hydrogenases, redox metalloenzymes with iron-iron (Fe-Fe), nickel-iron (NiFe), or iron-only (Fe) active sites (*3, 4*). Phylogenetic studies suggest that [Ni-Fe]-hydrogenases are the most ancestral (*4*); soluble nickel and iron ions were far more abundant in the Archean and Proterozoic oceans than today (*5, 6*). Extant hydrogenases are complex nanomachines (**Fig. 1**) that comprise hundreds of amino acids, multiple subunits, and multiple metal cofactors that ferry electrons to the active Ni-Fe site (*3*). However, the ancestral hydrogenase must have been much smaller and simpler. Model studies on a Ni-substituted rubredoxin show that a simple fold can evolve H_2 (*7*). Here, we demonstrate very short peptides can readily form di-nuclear nickel clusters capable of catalytically evolving H_2. Such peptides are simple enough that they could have emerged spontaneously during a prebiotic stage in the origin of life, giving rise to the first biotic metabolisms.

In extant [Ni-Fe]-hydrogenase, active site metal ions are coordinated by four cysteines, CN^-, CO and water (**Fig. 1, left**). The cysteines are separated by hundreds of amino acids, making it challenging to develop a minimal design that is directly analogous to the natural enzyme. Using naturally occurring minimal metal binding motifs (*8*) (**Fig. S1**), four cysteines were placed in a peptide scaffold with the pattern: **C**x**CGC**xxxxx**C**G. Remaining variable (x) positions were selected computationally using the structure-guided protein

design platform, protCAD (*9*), resulting in the Nickelback (NB) class of designs (see Supp. Methods for details). In the final design (**Fig. 1, center**), metal coordination mimicked features of the ACS di-nickel binding site (**Fig. 1, right**). As in ACS, a glycine (G4) and cysteine (C5) provide two backbone amides. Two sidechain thiols (C3, C5) complete the (distal) Ni^{2+} ion coordination with a square-planar geometry. C3 and C5 also serve as bridging ligands to a second (proximal) Ni^{2+} ion whose coordination is completed with the remaining cysteines C1 and C12. We define proximal/distal sites based on nomenclature from equivalent positions of nickels in ACS and hydrogenase. Coordinates for the DFT optimized model of NB-2Ni are provided (**Fig. S2**, Supp. Data).

Apo-NB was produced by Fmoc solid-phase synthesis and reconstituted with Ni^{2+} salts at 50^{o}C. Assembly was monitored by UV-visible absorption and circular dichroism (CD) spectroscopy (**Fig. 2A,C**). Two optically active species were identified: an assembly intermediate (2NB-1Ni) with the 2:1 (peptide:Ni) stoichiometry, and the final assembly (NB-2Ni) saturating at the 1:2 stoichiometry. Isosbestic points in the CD spectra (marked with arrows in **Fig. 2A**) support a direct conversion from 2NB-1Ni to NB-2Ni during the reconstitution. Spectral decomposition of the CD spectra with a two component model (**Figs. S5, S6**) was used to determine fractional concentrations of 2NB-1Ni and NB-2Ni during the course of the Ni reconstitution (**Fig. 2B**). The fully reconstituted NB-2Ni was confirmed to be stable at pH 5.5 to 10 and 20 to 90^{o}C (**Figs. S7, S8**), suggesting NB would have been stable over a range of predicted ocean pH and temperatures during the Archean eon (*10*).

In parallel with optical studies, we probed the redox activity of both the intermediate 2NB-1Ni and the mature NB-2Ni complexes using cyclic voltammetry (**Fig. 2D,S14-S16**). The catalytic current at -850 mV (vs SHE, standard hydrogen electrode) directly correlated with fraction of NB-2Ni species (**Fig. 2E**), confirming its electrochemical activity. This redox potential is more than sufficient to drive hydrogen evolution.

Catalytic H_2 production was demonstrated using a photochemical assay with an organic dye (EosinY) as a photosensitizer, and triethanolamine (TEOA) as a sacrificial electron donor, irradiated with green light using a 540 nm LED (*11*). H_2 evolution was quantified using gas chromatography. At pH 8, a turnover number TON = 500 and the turnover frequency TOF = 0.2 H_2/min were observed (**Fig. 2F**). Despite its small size, the TOF of NB is comparable to other Ni-binding designs (0.1-0.9 H_2/min), while the TON is substantially larger (*12, 13*).

These catalytic parameters could have provided sufficient energy to drive the first metabolisms of life (i.e. sulfate-, nitrate-, iron-reduction or methanogenesis). Assuming a peptide concentration of 10 nM, just a few molecules/cell, which is much lower than hydrogenase abundances in modern organisms (*14*), NB-2Ni could maintain a steady H_2 concentration of >20 nM (See Supp. Method for calculation). For comparison, active iron reducers in marine sediments have been observed at ~1 nM of [H_2] (*15, 16*). An NB-like peptide could have plausibly served as an electron source or sink in early metabolic pathways.

We probed the structure of the di-nickel site by EPR. The resting state of NB-2Ni is not EPR active, as both nickels are in the 2+ oxidation state. However, it was possible to trap one-electron reduced NB-2Ni in the presence of Eu(II)DTPA (*17*), and a small ligand, either CN^- or bicarbonate. EPR of the reduced state (**Figs. 3A and S17**) was characteristic of a d^9 electron configuration, with Ni^{1+} in distorted octahedral or square planar environment, and with the unpaired electron preferentially residing on a d_{x2-y2} orbital (*18, 19*). Both nickel sites have this coordination symmetry in our model structures. However, a distal site Ni^{1+} can be excluded because backbone amides would show up with strong hyperfine interactions, which were not observed in EPR/ESEEM experiments (**Figs. S17-25**). The reduced Ni^{1+} most likely occupies the proximal site (**Fig. 3C**). Similar Ni^{1+} EPR signatures have been reported for [NiFe]-hydrogenase (*20*) and the ACS proximal site (*21*) supporting the structural homology of NB-2Ni to these two enzymes (**Fig. 1**).

Conversely, oxidation of NB-2Ni with iridium chloride generated an Ni^{3+} EPR spectrum characteristic of a d^7 electron configuration with an unpaired electron residing on a d_{z2} orbital (*18, 19*), and with g-factor symmetry consistent with square-planar or elongated octahedral coordination (**Fig. 3B**). Remarkably, both the shape and the g-factor values of the oxidized NB-2Ni signal are very similar to oxidized nickel superoxide dismutase (Ni-SOD), where Ni^{3+} is in a square-pyramidal coordination with two backbone amides, two cysteines, and a histidine in the axial position (*22*). While NB does not contain

histidine, addition of 10 mM imidazole to oxidized NB-2Ni (**Fig. 3B** – red trace) recapitulated the ^{14}N hyperfine splitting seen in Ni-SOD, now resolved on the $g_{||}$ = 2.014 peak. This supports a Ni^{3+} at the distal position in the oxidized state (**Fig. 3C**).

If these Ni oxidation state assignments for the two sites are correct, removing C1 and C12 might eliminate the proximal site while retaining the distal one. We generated NBΔP with C1and C12 replaced by serine. Nickel titrations of NBΔP saturated at a 1:1 complex, with a different CD spectrum than NB-2Ni (**Fig. S10**). EPR of oxidized NBΔP-Ni is comparable with oxidized NB-2Ni (**Fig. S19**), confirming the assignment of Ni^{3+} at the distal site. No catalytic wave was observed for NBΔP-Ni in cyclic voltammetry (**Fig. S16**), indicating the distal Ni alone is insufficient for catalysis.

Many structural and chemical analogies exist between NB and ancient enzymes such as ACS (*23*), [Ni-Fe] hydrogenase, and accessory proteins for hydrogenase maturation (*24*). The chemical stability and functional potential of small peptides complexed with transition metals make them plausible ancestors in the evolution of oxidoreductases.

Acknowledgments. We thank G.C. Dismukes for providing access to the Bruker EPR Spectrometer.

Funding: NASA Astrobiology Institute Grant 80NSSC18M0093 (VN, PGF)

Authors Contributions. J.A.M., D.H.P., S.P., J.T., A.M.T., K.M.W., V.N., and P.G.F. designed research; J.A.M., D.H.P., S.P., J.T., A.M.T., P.M., J.S., J.J.M. performed research; J.A.M., D.H.P., S.P., J.T., A.M.T., P.M., J.S., J.J.M., K.M.W., R.L.K, V.N. and P.G.F. analyzed data; and J.A.M., D.H.P., S.P., J.T., A.M.T., V.N. and P.G.F. wrote the paper

Competing interests: Provisional Patent Application 63/257,464 – "A Minimal Catalytic D-Nickel Peptide Capable of Sustained Hydrogen Evolution and Methods of Use Thereof."

Data and materials availability. All data are available in the main text or the supplementary materials.

Supplementary Materials

Materials and Methods

Figs. S1 to S25

References (*25*–*77*)

Data S1

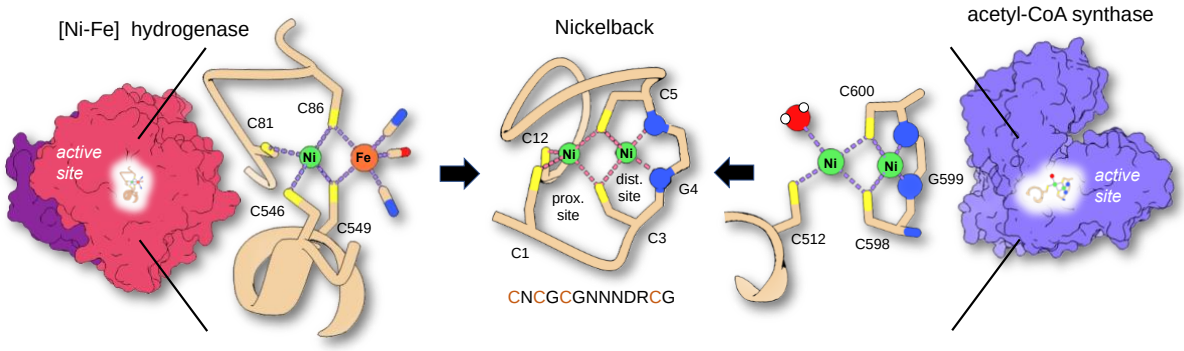

Figure 1. **Model structure of Nickelback (NB) and comparison to natural enzymes.** *Desulfovibrio* [Ni-Fe] hydrogenase (left, PDB ID: 5xle) and *Carboxydothermus* acetyl-CoA synthase (right, PDB ID: 1ru3) are large, complex proteins with active di-metal sites coordinated by a few ligands. The model structure of NB (center) combines elements of both active sites in a 13-residue polypeptide.

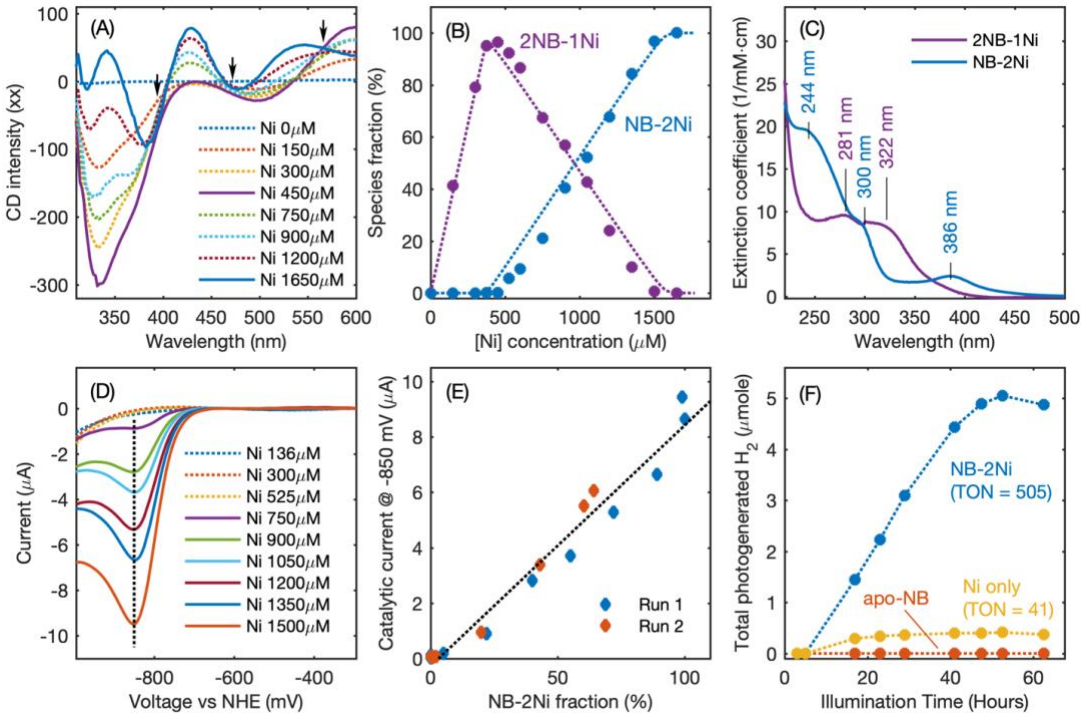

Figure 2. **Assembly and activity of NB. (A)** CD spectra of NB as a function of added Ni: [NB] = 750 μM, pH 7.5, temperature = 50 °C. The peak at 340 nm (assigned to 2NB-1Ni) at first grows reaching the maximum at [Ni] = 450 μM (solid purple line), and then declines at even higher [Ni] concentrations. The peak at 430 nm (assigned to NB-2Ni) starts to develop only at [Ni] > 500 μM and it grows monotonously to saturate around [Ni] = 1650 μM (solid blue line). Black arrows show isosbestic points. **(B)** Fractional concentrations of 2NB-1Ni and NB-2Ni as extracted from the two-component spectral decomposition of the CD spectra from panel A, as demonstrated in **Fig. S5, S6**. The dashed lines are the fits using a two-step reconstitution model: apo-NB → 2NB-1Ni → NB-2Ni (**Fig. S6**). The upper bounds for Ni^{2+} binding constants were estimated from the fit to be around 1 μM in both 2NB-1Ni and NB-2Ni. **(C)** Absorption spectra of pure 2NB-1Ni and NB-2Ni with characteristic bands labeled. **(D)** Reduction waves in bulk solution CV experiments at different stages of Ni reconstitution in NB: [NB] = 750 μM, pH 7.5, added [Ni] is indicated for each trace (Full traces in **Figs. S14-S16**). The catalytic current at -850 mV (vertical dashed line) starts to develop only at [Ni] > 500 μM and it grows linearly with the NB-2Ni fraction as demonstrated in **(E)**. **(F)** Photochemical H_2 evolution by NB-2Ni (10 μM) with EosinY (500 μM), TEOA (500 mM), 540 nm illumination, pH 8 at 37°C.

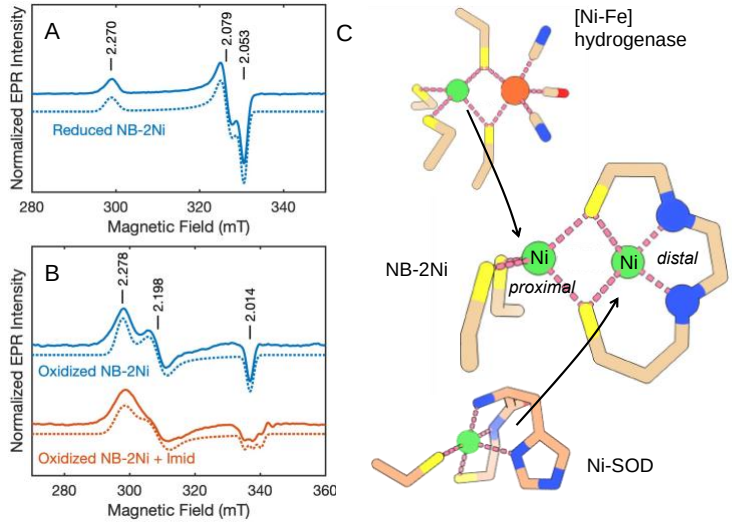

Figure 3. **Structural characterization of NB-2Ni.** EPR spectra of (A) reduced and (B) oxidized NB-2Ni at pH 10, measured at 20 and 30 K, respectively: (solid lines) experiment, and (dashed lines) EPR simulations. The principal g-factor values are marked with vertical lines and numbers. The oxidized NB-2Ni in (B) was measured in absence (blue traces) and presence (red traces) of imidazole ligands (10 mM). The g-factor symmetry of reduced (oxidized) NB-2Ni is similar to Ni^{1+} in [NiFe]-hydrogenase (blue dashed circle) and Ni^{3+} in Ni-SOD (red dashed circle), where Ni ions are found in distinctly different coordination sites, e.g. Ni^{1+} and Ni^{3+}, respectively. Both these Ni sites are represented in di-nickel NB-2Ni.

References

1. P. G. Falkowski, T. Fenchel, E. F. Delong, in *Science*. (American Association for the Advancement of Science, 2008), vol. 320, pp. 1034-1039.
2. K. H. Nealson, F. Inagaki, K. Takai, in *Trends in Microbiology*. (Elsevier Current Trends, 2005), vol. 13, pp. 405-410.
3. W. Lubitz, H. Ogata, O. Rüdiger, E. Reijerse, in *Chemical Reviews*. (American Chemical Society, 2014), vol. 114, pp. 4081-4148.
4. J. W. Peters *et al.*, in *Biochimica et Biophysica Acta (BBA) - Molecular Cell Research*. (Elsevier, 2015), vol. 1853, pp. 1350-1369.
5. H. Liu, K. O. Konhauser, L. J. Robbins, W.-d. Sun, Global continental volcanism controlled the evolution of the oceanic nickel reservoir. *Earth and Planetary Science Letters* **572**, 117116 (2021).
6. R. J. P. Williams, The bakerian lecture, 1981 natural selection of the chemical elements. *Proceedings of the Royal Society of London. Series B. Biological Sciences* **213**, 361-397 (1981).
7. J. Slater, W., S. C. Marguet, H. A. Monaco, H. S. Shafaat, in *Journal of the American Chemical Society*. (American Chemical Society, 2018), vol. 140, pp. 10250-10262.
8. O. Gutten, L. Rulíšek, in *Physical Chemistry Chemical Physics*. (The Royal Society of Chemistry, 2015), vol. 17, pp. 14393-14404.

9. D. H. Pike, V. Nanda, in *Biopolymers*. (NIH Public Access, 2015), vol. 104, pp. 360.

10. J. Krissansen-Totton, G. N. Arney, D. C. Catling, Constraining the climate and ocean pH of the early Earth with a geological carbon cycle model. *Proceedings of the National Academy of Sciences* **115**, 4105-4110 (2018).

11. A. Bachmeier, F. Armstrong, in *Current Opinion in Chemical Biology*. (Elsevier Current Trends, 2015), vol. 25, pp. 141-151.

12. M. J. Stevenson, S. C. Marguet, C. R. Schneider, H. S. Shafaat, in *ChemSusChem*. (John Wiley & Sons, Ltd, 2017), vol. 10, pp. 4424-4429.

13. D. Selvan *et al.*, in *ACS Catalysis*. (American Chemical Society, 2019), vol. 9, pp. 5847-5859.

14. K. Gutekunst *et al.*, In-vivo turnover frequency of the cyanobacterial NiFe-hydrogenase during photohydrogen production outperforms in-vitro systems. *Scientific reports* **8**, 1-10 (2018).

15. D. E. Canfield, E. Kristensen, B. Thamdrup, in *Advances in Marine Biology*. (Academic Press, 2005), vol. 48, pp. 65-94.

16. T. M. Hoehler, M. J. Alperin, D. B. Albert, C. S. Martens, in *Geochimica et Cosmochimica Acta*. (Pergamon, 1998), vol. 62, pp. 1745-1756.

17. K. A. Vincent *et al.*, Instantaneous, stoichiometric generation of powerfully reducing states of protein active sites using Eu (II) and polyaminocarboxylate ligands. *Chemical communications*, 2590-2591 (2003).

18. M. V. Gastel, W. Lubitz, in *Journal of the American Chemical Society*. (2009), pp. 441-470.

19. A. Abragam, B. B. Bleaney. (Oxford University Press, 2012), pp. 277-345.

20. M. E. Pandelia, H. Ogata, L. J. Currell, M. Flores, W. Lubitz, in *Biochimica et Biophysica Acta (BBA) - Bioenergetics*. (Elsevier, 2010), vol. 1797, pp. 304-313.

21. G. Bender *et al.*, in *Biochemistry*. (American Chemical Society, 2010), vol. 49, pp. 7516-7523.

22. D. P. Barondeau, C. J. Kassmann, Cami K. Bruns, a. John A. Tainer, E. D. Getzoff*, in *Biochemistry*. (American Chemical Society 2004), vol. 43, pp. 8038-8047.

23. E. Smith, H. J. Morowitz, in *Proceedings of the National Academy of Sciences*. (National Academy of Sciences, 2004), vol. 101, pp. 13168-13173.

24. K. C. Chan Chung *et al.*, A high-affinity metal-binding peptide from Escherichia coli HypB. *Journal of the American Chemical Society* **130**, 14056-14057 (2008).